A cycle jumping scheme for numerical integration of coupled damage and viscoplastic models for cyclic loading paths

Karim Nesnas — Khemais Saanouni

GSM/LASMIS, Université de Technologie de Troyes
B P 2060, 10010 Troyes cedex

ABSTRACT *A new practical methodology for the analysis of the damage to viscoplastic structures under low cycle fatigue loading paths is proposed The idea consists of carrying out a two time scale scheme an implicit algorithm for the numerical integration of the constitutive equations inside the loading cycles (small time scale), and an explicit scheme over the loading cycles (large time scale) For the small time integration, an implicit asymptotic algorithm based on the integral formulation of the constitutive equations, is used For the large time scale integration, an explicit algorithm, called "cycle jump technique" is used to integrate the model over all the loading cycles It can be shown that the combination of the two schemes is advantageous It allows to use and restore a limited number of variables, which are sufficient to estimate a cycle jump and give a measure of the way in which all the state variables are changing over the loading cycles Numerical results are presented and discussed at both Gauss point and structural levels in order to judge the applicability, efficiency and accuracy of the proposed method*

RÉSUMÉ *Une nouvelle méthodologie "pratique" de calcul des structures inélastiques endommageables sous chargements cycliques est proposée L'idée consiste à mettre au point un schéma à deux échelles de temps un algorithme implicite pour l'intégration numérique des équations de comportement à l'intérieur d'un cycle (temps court) et un algorithme explicite dans l'espace des cycles (temps long) Pour l'intégration sur le temps court, un algorithme asymptotique implicite a été développé, basé sur une formulation intégrale des relations de comportement endommageable Pour l'intégration sur le temps long, un algorithme explicite de saut de cycles est utilisé pour intégrer dans l'espace des cycles L'association de ces deux schémas présente des avantages utiliser et stocker un nombre restreint de variables, suffisantes pour estimer l'incrément de saut de cycles et donner une mesure adéquate de l'évolution de toutes les variables d'état le long des cycles Des résultats numériques sur un point de Gauss et des exemples soulignent l'applicabilité et l'efficacité de cette démarche*

KEY WORDS *viscoplasticity, damage, low cycle fatigue, asymptotic integration, cycle jump, finite elements*

MOTS CLÉS *Viscoplasticité, endommagement, fatigue à faible nombre de cycles, intégration asymptotique, saut de cycles, éléments finis*

Revue européenne des éléments finis. Volume 9 – n° 8/2000, pages 865 à 891

1. Introduction

The last two decades have shown an important progress in the derivation of constitutive equations. This is mainly due to the need for safety in many mechanical components subjected to very severe working conditions. For instance, structural components operating in nuclear or aerospace industries, are being subjected to increasingly severe and complex mechanical and thermal cyclic loading conditions. Such conditions often lead to a complex stress redistribution in structures, where localized regions of cyclic plasticity take place under cyclic thermal or mechanical loading paths. In addition, as discussed in [CHA 86], several processes interact i) the structural stress redistribution, ii) the cyclic hardening or softening processes which depend on the material and iii) the cyclic mean-stress relaxation which depends both on the material and on the applied loading.

Moreover, the stress redistribution is also due to the interaction and cumulation of many kinds of material deterioration (such as ductile, creep and fatigue damages), which induce a non-homogeneous distribution of the material properties, when combined with different mechanical behavior (elasticity, plasticity and viscoplasticity...). This may have a great influence on the residual life of the structures. In other words, it is necessary to model the complete strain and damage behavior of the material in order to make an accurate failure analysis of structure (evaluation of the lifetime). This is possible with the classical elasto-viscoplastic constitutive equations "strongly" coupled to the damage evolution equations.

Usually, the fatigue life prediction (high and low cycle fatigue) is made using simplified uncoupled approaches ([BEN 81], [LEM 86] and [AKR 97]). The principle is to calculate the mechanical fields distribution within the structure for one typical loading cycle (generally the so called stabilized cycle) Then, the obtained solution is used to predict the fatigue-life of each material (or Gauss) point of the structure. This uncoupled approach, even if it is very easy to use, cannot take into account the distribution of the mechanical fields due to their different interactions This leads us to underestimate the fatigue life according to the non relaxation of the stresses under the effect of the damage initiation and growth

The fully coupled approach, developed in this work, allows to take into account accurately both transient stages of the fatigue life: (i) the positive hardening at the beginning of the loading history, (ii) the negative hardening observed during the last loading cycles due to the damage growth until the initiation of the macroscopic crack. Consequently, this kind of approach, if more expensive than the previous one, is thought to predict more accurately when and where the fatigue damage initiation can take place within geometrically complex structures.

On the other hand, the coupled constitutive equations governing the evolution of internal state variables are, in general, highly non-linear and mathematically 'stiff'. This inherent stiff character of the constitutive equations causes major problems during numerical integration. Present-day, structural engineering problems involve

complex thermal and mechanical loading histories, especially the case of cyclic loading. For the solution of these problems, the entire loading history has to be traced, requiring these equations to be integrated many times. The cost and CPU time involved abandoning the conventional methods of employing small time steps over the total fatigue life for accurate integration of these stiff equations. Therefore, there is a strong need to develop efficient and accurate integration algorithms with a self-adaptative time-step strategy that can achieve the desired accuracy and stability over the entire integration range *i e.* the loading history (many thousand cycles).

Keeping the aforementioned requirement in mind, a great deal of study on numerical methods for integrating damage and/or viscoplastic rate equations in relation to the solution of boundary value problems has been reported Several numerical schemes have proven to be quite effective. In general terms, it has been argued that even if the multi-step methods such as those due to [GEA 81] usually give better solution accuracy as well as reliability, they are not suitable for large-scale finite element computation because of their excessive need for computer storage. In view of this, one-step integration methods are much more desirable. In the context of these latter methods, two classes of algorithms can be identified: explicit and implicit algorithms. Extensive discussions on the advantages and disadvantages of these methods are available in the following works ([SIM 86], [GOL 89], [GEL 92], [TOU 93]...). More recently, some works ([FRE 92], [CHU 91]) have proposed explicit and implicit asymptotic exponential integration algorithms with application to the integration of viscoplastic models. Unfortunately, the calculation of a large number of successive loading cycles between the initial undamaged and the final fully damaged (initiation of a macroscopic crack) states is still very expensive. For that reason, some methods have been developed to make possible the structure computation over a large number of cycles The so called "large time increment algorithm" [LAD 85] and "the time homogenization method" ([GUE 86]) can be considered as straightforward methods to achieve this task However, some engineering approaches have been proposed to increase the efficiency and the usefulness of these methods Their main objective is to realize some cycle jumping increments using explicit schemes [LEN 89], [DUN 94] and [NES 98].

In the present paper, the damaged viscoplastic model is implemented in both the in-house point material solver as well as the general purpose finite element code SIC (available at the University of Technology of Compiègne). A two time scale integration scheme is proposed. It uses, (i) an implicit asymptotic algorithm for the numerical integration in the time space, and (ii) an explicit cycle jump algorithm in the cycle space. This allows the numerical prediction of the fatigue life of mechanical components. The main advantage of this scheme is to reduce the number of variables in both scales. Numerical results are presented and discussed in order to judge the applicability, efficiency and accuracy of this integration strategy in conjunction with the damaged viscoplastic model.

2. Coupled Damage and viscoplastic constitutive equations

The classical framework of thermodynamics of irreversible processes with internal state variables is used. The present phenomenological model takes into account both non-linear hardening (isotropic and kinematic) and isotropic damage as dissipative phenomena. For the sake of simplicity only the small strain isothermal transformations are considered. This leads to neglect of the heat transfer and to assuming the additive decomposition of the total strain according to $\varepsilon_{ij} = \varepsilon^e_{ij} + \varepsilon^p_{ij}$. Here, ε^p_{ij} represents the overall plastic and viscoplastic strain components. The thermodynamic formalism is based on the assumption of the existence of two potentials depending on the state variables. These are, classically, divided into two families·

– the controlled or observable state variables reduced in this isothermal case to the total strain tensor associated to the Cauchy stress tensor $(\varepsilon_{ij},\sigma_{ij})$

– the non observable or internal state variables taken here as :

- the isotropic hardening variables (r,R)
- the kinematic hardening represented by k internal variables (α^k_{ij},X^k_{ij}).
- the isotropic damage variables (D,Y).

The coupling between damage and viscoplastic behavior is carried out through the effective state variables which can be used in the state and dissipation potentials instead of the classical state variables defined above. In this work, these effective state variables are determined by using the hypothesis of the total energy equivalence [SAA 94]. Therefore, the relationship between the effective and the classical state variables are chosen as:

$$\tilde{\varepsilon}^e_{ij} = \sqrt{1\text{-}D}\ \varepsilon^e_{ij} \quad , \quad \tilde{\sigma}_{ij} = \frac{\sigma_{ij}}{\sqrt{1\text{-}D}} \tag{1}$$

$$\tilde{r} = \sqrt{1\text{-}D}\ r \quad , \quad \tilde{R} = \frac{R}{\sqrt{1\text{-}D}} \tag{2}$$

$$\tilde{\alpha}^k_{ij} = \sqrt{1\text{-}D}\ \alpha^k_{ij} \quad , \quad \tilde{X}^k_{ij} = \frac{X^k_{ij}}{\sqrt{1\text{-}D}} \tag{3}$$

2.1. *The state equations*

The fully coupled state laws are summarized hereafter (see [SAA 94] for more details).

$$\sigma_{ij} = \frac{\nu\tilde{E}}{(1+\nu)(1-2\nu)}\varepsilon^e_{kk}\delta_{ij} + \frac{\tilde{E}}{(1+\nu)}\varepsilon^e_{ij} \tag{4}$$

$$X_{ij}^k = \frac{2}{3}\widetilde{C}_k\,\alpha_{ij}^k \tag{5}$$

$$R = \widetilde{Q}r \tag{6}$$

$$Y = Y_\varepsilon + Y_\alpha + Y_r \tag{7}$$

$$Y_\varepsilon = \frac{1}{2}\frac{J_2^2(\widetilde{\sigma}_{ij})}{\widetilde{E}}\sigma^* \tag{7a}$$

$$Y_\alpha = \frac{1}{2}\sum_{k=1}^{n}\frac{J_2^2(\widetilde{X}_{ij}^k)}{\widetilde{C}_k} \tag{7b}$$

$$Y_r = \frac{1}{2}\frac{\widetilde{R}^2}{\widetilde{Q}} \tag{7c}$$

In these equations δ_{ij} denotes the second order unit tensor, E and ν are respectively the Young modulus and Poisson's ratio. The elastic, kinematic and isotropic moduli in the damaged state are respectively defined by. $\widetilde{E} = (1\text{-}D)E$, $\widetilde{C}_k = (1\text{-}D)C_k$ and $\widetilde{Q} = (1\text{-}D)Q$, where C_k is the k^{th} kinematic hardening modulus and Q the isotropic hardening modulus. The invariant $J_2(Z_{ij})$ defines, in the stress space and for any symmetric second order tensor Z_{ij}, the following norm :

$$J_2(Z_{ij}) = \sqrt{\frac{3}{2}Z_{ij}^D Z_{ij}^D} \tag{8a}$$

where $Z_{ij}^D = Z_{ij} - \frac{1}{3}Z_{kk}\,\delta_{ij}$ is the deviatoric part of Z_{ij} In Eq (7a), σ^* is the multiaxial damaged criterion defined by .

$$\sigma^* = \frac{2}{3}(1+\nu) + 3(1-2\nu)\left(\frac{\sigma_H}{J_2(\sigma_{ij})}\right)^2 \tag{8b}$$

σ_H being the hydrostatic pressure.

Note that the translation of the yield surface center, i.e. the kinematic hardening effect, is given by the sum of the overall X_{ij}^k tensors:

$$X_{ij} = \sum_k X_{ij}^k \tag{8c}$$

2.2. Evolution equations: Differential formulation

The evolution equations associated to the dissipative phenomena are deduced from appropriated yield function and dissipation potential. For the isothermal case, one get [SAA 94]:

$$\dot{\varepsilon}^p_{ij} = \dot{\tilde{\lambda}}_p \, n_{ij} \,, \qquad n_{ij} = \frac{3}{2} \frac{\sigma^D_{ij} - X_{ij}}{J_2(\sigma_{ij} - X_{ij})} \tag{9}$$

$$\dot{\alpha}^k_{ij} = \dot{\varepsilon}^p_{ij} - a_k \dot{\lambda}_p \, \alpha^k_{ij} \tag{10}$$

$$\dot{r} = \dot{\tilde{\lambda}}_p \, (1 - b \, \tilde{r}) \tag{11}$$

$$\dot{D} = \lambda_p \frac{\sigma^*(p-p_i)^\gamma}{\Gamma} \frac{1}{(1-D)^\eta} \tag{12}$$

where a_k and b are material coefficients characterizing the non-linearity of the hardening; γ, Γ and η are material coefficients characterizing the damage evolution and p_i being the value of p at the beginning of the i^{th} loading cycle. n_{ij} is the normal to the yield surface.

The viscoplastic « multiplier » $\dot{\lambda}_p$ is given by:

$$\dot{\lambda}_p = \left(\frac{J(\tilde{\sigma}_{ij} - \tilde{X}_{ij}) - \tilde{R} - k}{K} \right)^N \tag{13}$$

and

$$\dot{\tilde{\lambda}}_p = \frac{\dot{\lambda}_p}{\sqrt{1-D}} \tag{14}$$

with K and N are viscosity parameters and k is the initial yield surface radius.

It can be seen that $\dot{\lambda}_p$ is nothing but the norm of the plastic strain rate defined by:

$$\dot{\tilde{\lambda}}_p = \dot{p} = \sqrt{\frac{2}{3} \dot{\varepsilon}^p_{ij} \dot{\varepsilon}^p_{ij}} \tag{15}$$

The damage evolution law is chosen through equation (12) to represent, in this work, the low cycle fatigue mechanism ([LEM 86]) . Moreover, the thermodynamic admissibility of the present model can be easily shown ([SAA 94]).

2.3. *Evolution equations: Integral formulation*

The set of constitutive equations ((9) to (12)) forms a system of highly non-linear first order ordinary differential equations (ode) defined at a given time They can be integrated numerically using a classical explicit or implicit integration schemes According to the original work (without damage) by [WAL 87], it is possible to convert these ode into a new set of integral equations defined over an interval of time Applied to the fully coupled constitutive equations presented above, one may get [NES 98]:

$$\sigma_{ij}(t) = X_{ij}(t) + \frac{\nu E}{(1+\nu)(1-2\nu)}\varepsilon_{kk}(t)\delta_{ij} + \int_{\xi=0}^{t} \exp\left\{-(L(t)-L(\xi))\right\} \times \left(2\mu\frac{\varepsilon_{ij}}{\xi} - \frac{2\mu}{3}\frac{\varepsilon_{kk}}{\xi}\delta_{ij} - \frac{X_{ij}}{\xi}\right)d\xi \tag{16}$$

$$\alpha_{ij}^{k}(t) = \int_{\xi=0}^{t} \exp\left\{-(G^{k}(t)-G^{k}(\xi))\right\}\frac{\varepsilon_{ij}^{p}}{\xi}d\xi \tag{17}$$

$$r(t) = \int_{\xi=0}^{t} \exp\left\{-(Q(t)-Q(\xi))\right\}\frac{p}{\xi}d\xi \tag{18}$$

$$D = \int_{0}^{t}\left(\left[\frac{\sigma^{*}(p-p_i)^{\gamma}}{\Gamma}\right]\frac{1}{(1-D)^{\eta}}\frac{p}{\xi}\right)d\xi \tag{19}$$

with:

$$L(t) = \int_{\xi=0}^{t}\left(\frac{3\tilde{\mu}\,(\partial p/\partial\xi)}{K\sqrt{1-D}\left(\sqrt{1-D}\,p\right)^{1/N} + \tilde{Q}r + \sqrt{1-D}k} + \frac{D}{\xi}\frac{1}{1-D}\right)d\xi \tag{20}$$

$$G^{k}(t) = \int_{\xi=0}^{t} a_k\sqrt{1-D}\,\frac{p}{\xi}d\xi \tag{21}$$

$$Q(t) = \int_{\xi=0}^{t} b\sqrt{1-D}\,\frac{p}{\xi}d\xi \tag{22}$$

The state variables are now expressed in the form of implicit recursive integral equations (Eq. (16) to (19)), which depend on the scalar parameters L, G^k and Q which are themselves integral functions as indicated by Eq. (20) to (22) All these developments can be found in [NES 98] and will be published in a forthcoming paper [NES 00].

3. A two time scale integration scheme for cyclic loading

This section is devoted to the presentation of a new methodology for the integration of the coupled damage viscoplastic constitutive equations under cyclic loading paths This procedure uses: (i) an implicit asymptotic algorithm to the numerical integration in the time space (small time scale) and (ii) an explicit algorithm (cycle jumping technique) in the cycle space (large time scale) It will be shown the advantage of the association of the two schemes in reducing the number of variables to integrate the constitutive equations. In fact, the small time integration scheme involves only a resolution of two non-linear equations While the large time integration scheme can be used with only two variables which are sufficient to estimate the cycle jump step (ΔN). This gives a convenient measure of the way in which all state variables are changing over the cycling history

3.1. *Small time scale integration*

A number of numerical integration schemes are available for numerical integration of the ordinary differential equations. The choice of a particular scheme is dominated by four considerations: i) stability, ii) convergence, iii) suitability for finite element implementation, and iv) computational cost. In the following, a numerical time integration is performed by an asymptotic integration algorithm initially proposed by [WAL 87] and extended in [NES 00] to the coupled damage and viscoplastic models described in the previous section. The algorithm is based on the approximation of the set of integrals Eq (16) to (19) using a recursive relationship In order to evaluate these integrals, an asymptotic expansion of the related integrand is performed about the upper limit of the time interval [t, $t+\Delta t$], resulting in an iterative implicit integration scheme Similarly to the classical algorithm ([AUR 94], [CHAB 96] and others), the asymptotic scheme reduces the fully coupled equation to two scalar equations in the case of fully isotropic flow (plasticity and damage). Initial anisotropy needs, at least, two additional tensorial equations for both plasticity and damage flow ([HAM 00]). However, the asymptotic algorithm can not be applied for initial anisotrpy related to the plasticity, since parameters L, G^k and Q have to be scalars. Within a typical time step [t, $t+\Delta t$], one can obtain the above integral Eq. (16) to (19) in term of the appropriate variables value defined at the beginning of the current time step. With the resulting integrated form of each state variables, the asymptotic expansion can

now be used to represent each integral. Therefore, the specific relations associated to each physical quantity (Cauchy stress, kinematic hardening, isotropic hardening and damage variables) are given by [NES 98]:

Cauchy stress

$$\begin{aligned}\sigma_{ij}(t+\Delta t) = X_{ij}(t+\Delta t) &+ \frac{\nu\tilde{E}}{(1+\nu)(1-2\nu)}\varepsilon_{kk}(t)\delta_{ij} \\ &+ \exp\left\{-\Delta L\right\}\left[\sigma_{ij}(t) - X_{ij}(t) - \frac{\nu\tilde{E}}{(1+\nu)(1-2\nu)}\varepsilon_{kk}(t)\delta_{ij}\right] \\ &+ \left(2\tilde{\mu}\Delta\varepsilon_{ij} - \frac{2\tilde{\mu}}{3}\Delta\varepsilon_{kk}\delta_{ij} - \Delta X_{ij} - \frac{\Delta D}{1-D}X_{ij}\right)\left[\frac{1-\exp(-\Delta L)}{\Delta L}\right]\end{aligned} \tag{23}$$

with

$$\Delta L = \frac{3\tilde{\mu}\Delta p}{K\sqrt{1-D}\left(\sqrt{1-D}\,\Delta p/\Delta t\right)^{1/N} + \tilde{Q}\,r(t+\Delta t) + \sqrt{1-D}k)} + \frac{\Delta D}{1-D} \tag{24}$$

Kinematic hardening

$$\alpha_{ij}^{k}(t+\Delta t) = \exp\left\{-\Delta G^{k}\right\}\alpha_{ij}(t) + \Delta\varepsilon_{ij}^{p}\left[\frac{1-\exp(-\Delta G^{k})}{\Delta G^{k}}\right] \tag{25}$$

with:

$$\Delta G^{k} = a_k\sqrt{1-D}\,\Delta p \tag{26}$$

Isotropic hardening.

$$r(t+\Delta t) = \exp\left\{-\Delta Q\right\}r(t) + \Delta p\left[\frac{1-\exp(-\Delta Q)}{\Delta Q}\right] \tag{27}$$

with.

$$\Delta Q = b\sqrt{1-D}\,\Delta p \tag{28}$$

Damage

Two time discretisation schemes can be used:

– first order approximation:

$$D(t + \Delta t) = D(t) + \Delta D = D(t) + \dot{D}(t+\Delta t)\,\Delta t \tag{29}$$

– second order approximation:

$$D(t + \Delta t) = D(t) + \Delta D = D(t) + 0.5\,(\dot{D}(t) + \dot{D}(t+\Delta t))\,\Delta t \tag{30}$$

The recursive relationships given in Eq. (23), (25), (27) and (29) or (30) for determining $\sigma_{ij}(t+\Delta t)$, $\alpha_{ij}^{k}(t+\Delta t)$, $r(t+\Delta t)$ and $D(t+\Delta t)$ involve the parameters ΔL, ΔG^{k}, ΔQ and ΔD. These parameters, in turn, via equations (24), (26) and (28), require a knowledge of $\sigma_{ij}(t+\Delta t)$, $\alpha_{ij}^{k}(t+\Delta t)$, $r(t+\Delta t)$ and $D(t+\Delta t)$, for their evaluation. These equations are then recursive or implicit equations. Therefore, four implicit equations have to be resolved by Newton-Raphson iterative method However, the parameters ΔL and ΔQ are linearly dependent and related to the cumulated plastic strain $\Delta p = \dot{p}(t+\Delta t)\,\Delta t$. One can evaluate these parameters by computing the second invariant of the plastic strain rate, using.

$$\Delta\varepsilon_{ij}^{p} = \Delta e_{ij} - \Delta s_{ij}/\,2\,\tilde{\mu} - \Delta D s_{ij}\,/2\,\tilde{\mu}(1 - D) \tag{31}$$

where Δe_{ij} is deviatoric strain tensor increment and μ is the shear modulus in the damaged state ($\tilde{\mu} = (1\text{-}D)\mu$).

The unknowns are then reduced to ΔL and ΔD, which can be determined by the resolution of the following implicit nonlinear system (two equations):

$$g_1(\Delta L, \Delta D) = \Delta L - \frac{3\tilde{\mu}\Delta p}{K\sqrt{1\text{-}D}\left(\sqrt{1\text{-}D}\;\Delta p/\Delta t\right)^{1/N} + \tilde{Q}r(t+\Delta t) + \sqrt{1\text{-}D}k)} - \frac{\Delta D}{1\text{-}D} = 0 \tag{32}$$

and

$$g_2(\Delta L, \Delta D) = \Delta D - \dot{D}(t+\Delta t)\,\Delta t = 0 \tag{33a}$$

or

$$g_2(\Delta L, \Delta D) = \Delta D - 0.5\,(\dot{D}(t)+\dot{D}(t+\Delta t))\,\Delta t = 0 \tag{33b}$$

If $\Delta L = x_1$ and $\Delta D = x_2$, then equations (32) and (33a) or (33b) can be written as:

$$g_i(x_j) = 0 \tag{34}$$

Using the classical Taylor expansion of the functional g_i, the equation (34) can be linearized to get:

$$\frac{g_i(x_j^k)}{x_j}\,\delta x_j^k = -\,g_i(x_j^k) \tag{35}$$

Each step of the iteration procedure requires the solution of (32). For δx_j^k, which defines a new intermediate solution x_j^{k+1}:

$$x_j^{k+1} = x_j^k + \delta x_j^k \tag{36}$$

being the basis of the next iteration step. This iterative process is continuated until convergence toward the solution, when the following convergence criteria are satisfied:

$$\frac{\left\|\delta x_j^k\right\|_2}{\left\|\delta x_j^1\right\|_2} \le \varepsilon_1 \qquad \text{and} \qquad \frac{\left\|\delta g_j^k\right\|_2}{\left\|\delta g_j^1\right\|_2} \le \varepsilon_2 \tag{37}$$

where ε_1 and ε_2 are tolerance limits ($\varepsilon_1 = \varepsilon_2 = 10^{-4}$) and $\|\bullet\|_2$ designates an Euclidean norm From a computational standpoint, the asymptotic integration algorithm appears to be quite appealing. In (36), the coefficient matrix, denoted by $J = \partial g_i/\partial x_j$, a 2x2 Jacobian matrix may be derived analytically or numerically. The efficiency and performance of this scheme is compared to others in [NES 98] or [NES 00].

3.2. *A large time scale integration*

The treatment of the numerical integration in the case of cyclic loading paths must be involved by using an appropriate scheme, which is adapted to the behavior of the structure in the cycle space (Figure 1). In fact, the fatigue life of the structure can be schematically decomposed into three main stages· i) the hardening stage where the maximum stress (pick stress value for each cycle) increases, ii) the stabilized stage, defined as the stage in which the internal stresses are in equilibrium with the damage effects and finally iii) the softening stage represented by the decreasing of the stress fields due to the rapid increasing of damage until final fracture It is obvious that the stabilized stage represents the longest stage of the lifetime, especially in the case of high cycle fatigue. Therefore, it is often impossible to make the simulation of the behavior of the structure during all its lifetime. An accelerated calculation method, called "cycle jump technique" initially proposed by ONERA [LEN 89] and used by [DUN 94] and [NES 98], seems to be more attractive for its simplicity of implementation in general purpose finite element codes.

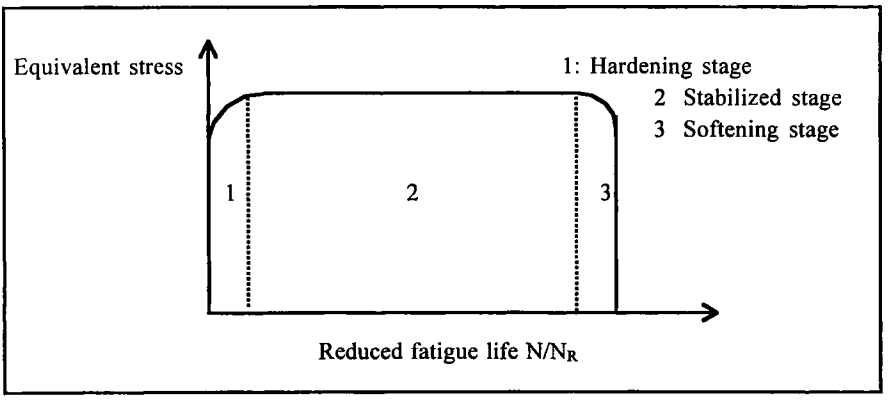

Figure 1. *Schematic representation of of the fatigue life main stages*

The principle of this technique is based on the fact that for large time part of the structure lifetime (stabilized stage), stress redistribution is small This suggests a possibility to drop the calculation of some intermediate cycles. In order to do this, it is necessary to express the vector y containing the state variables as a cycle function instead of a time function. Therefore, a particular cycle instant τ ($0 \leq \tau \leq T$) during the N^{th} cycle is chosen so that the value of the vector at this cycle is given by:

$$\mathbf{y}(N) = \mathbf{y}((N-1)T + \tau) \tag{38}$$

where T is the cycle period. The problem reduces then to find a succession of discrete values for the y_N:

$$\mathbf{y}(0 \leq N \leq N_R) \tag{39}$$

where N_R represents the number of cycles to failure.The integration of the variable y_N is performed by using a second order Taylor expansion as follows.

$$\mathbf{y}_{N+\Delta N} = \mathbf{y}_N + \dot{\mathbf{y}}_N \Delta N + \ddot{\mathbf{y}}_N \frac{\Delta N^2}{2} + . \tag{40}$$

The rate change of the state variables $\dot{y}_N$ is expressed in term of a "pseudo" differential equation defined as follow:

$$\dot{\mathbf{y}}_N = \frac{\delta \mathbf{y}}{\delta N} = \frac{\mathbf{y}_{N+1} - \mathbf{y}_N}{1} \tag{41}$$

The second derivative $\ddot{y}_N$ is also expressed approximately in term of the state variables rate $\dot{y}_N$ The cycle jump length DN can be determined such that the error, resulting from truncating the higher order terms, is lower than a fixed tolerance η. The procedure for obtaining ΔN from the rate of change of the state variables is outlined using two possibilities. The first one consists in limiting the Taylor expansion to the first order and calculate an optimal cycle jump ΔN which keep sufficiently small the first order term compared with the actual value

$$\left|\ddot{y}_N\right| \Delta N \leq \eta_1 \left|y_N\right| \;\Rightarrow\; \Delta N = \eta_1 \frac{\left|y_N\right|}{\left|\ddot{y}_N\right|} \tag{42}$$

where η_1 is an accuracy parameter. The second possibility is a second order Taylor development where the optimal ΔN step results from the minimization of the second order term comparing to the first order one with an h_2 accuracy parameter

$$\left|\dddot{y}_N\right| \frac{\Delta N^2}{2} \leq \eta_2 \left|\dot{y}_N\right| \Delta N \;\Rightarrow\; \Delta N = 2\,\eta_2 \frac{\left|\dot{y}_N\right|}{\left|\dddot{y}_N\right|} \tag{43}$$

The cycle jump increment ΔN is evaluated for each state variables at each integration point of the structure. The selected value is the minimum one among all ΔN_i

The classical jump technique uses all the state variables to estimate the cycle jump length. These latter change differently (more or less non-linear) with different levels. This leads to difficulties to determine the suitable value of the cycle jump, particularly, when a cycle jump value belonging to state variables with insignificant values are taken into account. In order to establish a general approach for the determination of a suitable cycle jump increment (ΔN), it is necessary to choose suitable parameters which give a measure of the way in which all state variables are changing. New parameters given by the integral formulation of the problem may be considered as adequate variables describing the different stages of the evolution in the cycle space of the state variables. For instance, the parameter ΔL has an important role in the asymptotic algorithm. It is an increment quantity over a given time step, which appears in the implicit recursive expression of the integral equation associated to the stress tensor. This expression gives not only the stress tensor at the end of time step, but take into account the rotation of the flow direction (i e the normal to the yield surface) during the non-proportional loading paths. Moreover, as schown in Figure 2, the parameter ΔL is sensitive to the main non-linearities of the model during both the hardening and the softening stages for any proportional and non proportional loading paths including the continuous rotation of the normal to the yield surface. This suggests the use of the parameter ΔL as a main parameter to

estimate the cycle jump ΔN using (42) or (43). However, to enhance the calculation of ΔN during the softening stage, the damage variable D (or its increment ΔD) can be helpfully used

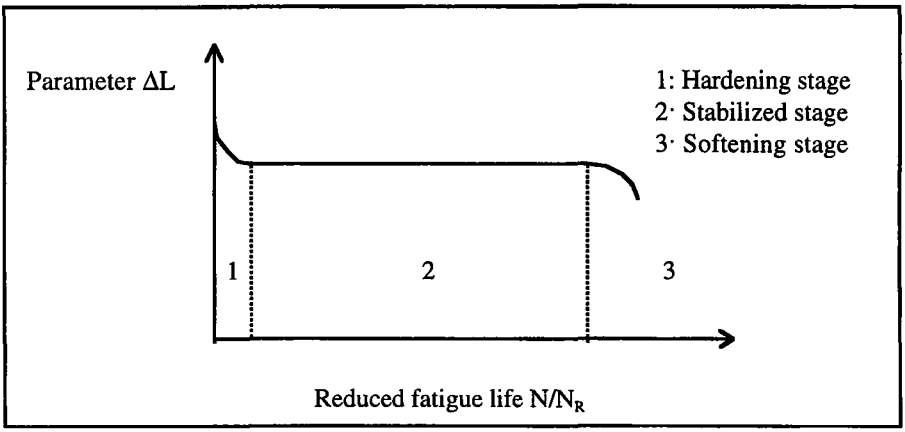

Figure 2. *Shematic evolution of ΔL over the cycles*

Consequently, the cycle jump method can work as follow:

(i) after each cycle jump, the constitutive equations are numerically integrated over a given number of cycles (5 cycles for instance) This ensures the stability of the solution before the next jump and permits to estimate the needed pseudo-derivatives.

(ii) compute the first and second pseudo-derivatives, at the same time, necessary to determine the cycle jump increment ΔN, which is needed for the state variables extrapolation.

(iii) calculate the cycle jump for the two variables ΔL and D with the following relation:

$$\Delta N_{\Delta L} = \eta \frac{\Delta L}{\dot{\Delta L}} \text{ and } \Delta N_D = \eta \frac{D}{\dot{D}} \Rightarrow \Delta N = \min(\Delta N_{\Delta L}, \Delta N_D) \qquad (44)$$

(iv) extrapolate the state variables by considering two cases·

– first scheme (noted CJTV1 as the Cycle Jump Technique Version 1) the extrapolation for ΔN cycles is made for all state variables with the Taylor development Eq. (40),

– second scheme (noted CJTV2 as the Cycle Jump Technique Version 2) the extrapolation is made on the parameters ΔL, Δp and D with Eq. (40). The results

are then substituted in the asymptotic forms Eqs. (23), (25) and (27), which give the extrapolation of the remaining the state variables.

$$\sigma_{ij}^{N+\Delta N}(t+\Delta t) = \frac{2}{3}\widetilde{C}\,\alpha_{ij}^{N+\Delta N}(t+\Delta t) + \frac{\nu\widetilde{E}}{(1+\nu)(1-2\nu)}\varepsilon_{kk}(t+\Delta t)\delta_{ij}$$

$$+ \exp\left\{-\Delta L_{N+\Delta N}\right\}\left[\sigma_{ij}^{N}(t) - \frac{2}{3}\widetilde{C}\,\alpha_{ij}^{N}(t) - \frac{\nu\widetilde{E}}{(1+\nu)(1-2\nu)}\varepsilon_{kk}(t)\delta_{ij}\right] \qquad (45)$$

$$+ \left(2\widetilde{\mu}\Delta\varepsilon_{ij} - \frac{2\widetilde{\mu}}{3}\Delta\varepsilon_{kk}\delta_{ij} - \frac{2}{3}\widetilde{C}\,\Delta\alpha_{ij} - \frac{2}{3}\widetilde{C}\frac{\Delta D}{1-D_{N+\Delta N}}\alpha_{ij}\right)\left[\frac{1-\exp(-\Delta L_{N+\Delta N})}{\Delta L_{N+\Delta N}}\right]$$

$$\alpha_{ij}^{kN+\Delta N}(t+\Delta t) = \exp\left\{-\Delta G_{N+\Delta N}^{k}\right\}\alpha_{ij}^{kN}(t) + \Delta\varepsilon_{ij}^{p}\left[\frac{1-\exp(-\Delta G_{N+\Delta N}^{k})}{\Delta G_{N+\Delta N}^{k}}\right] \qquad (46)$$

$$r^{N+\Delta N}(t+\Delta t) = \exp\left\{-\Delta Q_{N+\Delta N}\right\} r^{N}(t) + \frac{\Delta p_{N+\Delta N}}{\sqrt{1-D_{N+\Delta N}}}\left[\frac{1-\exp(-\Delta Q_{N+\Delta N})}{\Delta Q_{N+\Delta N}}\right] \qquad (47)$$

with

$$\Delta Q_{N+\Delta N} = b\Delta p_{N+\Delta N} \text{ and } \Delta G_{N+\Delta N}^{k} = a_k\,\Delta p_{N+\Delta N}$$

The cycle jumping technique presented above is used to predict the response of a material point or structural components submitted to cyclic mechanical loading paths. The results are compared with those obtained by carrying out the complete computations over all the loading cycles without cycle jumping. The effectiveness and accuracy of the cycle jumping technique can therefore be evaluated.

4. Numerical examples

Numerical examples, in both Gauss point and structural levels, are given to demonstrate the utility of the proposed numerical schemes. Several aspects are illustrated through these examples namely accuracy, convergence and applicability in structural analysis. All computer runs were made on the DEC ALPHA 3000 workstation Some fixed parameters are introduced in the implementation of the cycle jump technique·

– the time t in the cycle which gives the large time value of the state variables,

– the minimum number of cycles (JUMPMIN) to compute successively before to jump;

– the accuracy parameters h for the cycle jump step ΔN;

– the authorized maximum number of jump cycles (JUMPMAX).

The material parameters adopted in the subsequent numerical studies are compiled in Table 1.

	Parameter	Value	Unit
- Isotropic elasticity	E	144000	MPa
	ν	0 3	-
- Viscosity	N	10	-
	K	2000	MPa
- Yield stress	k	211	MPa
- Isotropic hardening	Q	3000	MPa
	b	10 or 3	-
- Kinematic hardening	C	10000	MPa
	a	20 or 5	-
- Fatigue damage	γ	0 3	-
	Γ	12	-
	η	15	-

Table 1. *Used material parameters*

4.1. *At Gauss point level*

In this section, some numerical simulations are carried out using two typical biaxial loading paths The first one (Figure 3a) is isochoric and proportional inducing a constant normal to the yield surface The second one (Figure 3b) is non proportional inducing four changes of the normal to the yield surface during one loading cycle. The chosen τ is the end of sequence 1 in Figure 3a and 2 in Figure 3b (located by a star). The adopted values of JUMPMIN and JUMPMAX are respectively 5 and 60 cycles.

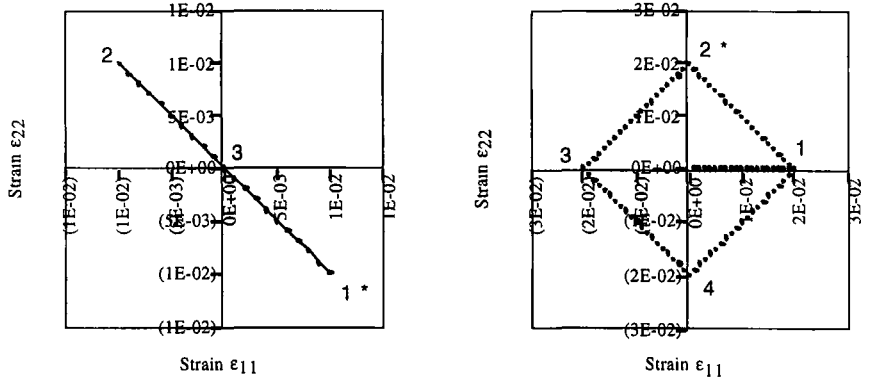

(a) (b)

Figure 3. *Selected a) proportional and b) non-proportional loading paths*

The first verification of the cycle jump technique, with the two schemes CJTV1 and CJTV2 described in section 3, concerns the convergence. Figures 4 and 5 represent the evolution of the maximum equivalent stress (peak stress value for each cycle) versus the reduced fatigue life (N/N_R), for both cycle jump techniques (shown by symbols) and full calculations over all cycles (shown by solid line) The solution obtained by the complete cycle by cycle calculation (solid line curve) is taken as a reference solution which gives a total fatigue life $N_R = 384$ cycles The fatigue lives obtained with the proposed cycle jump scheme are:

* CJTV1: For $\eta = 0.01$, only 134 cycles have been calculated giving a total fatigue life of $N_R = 389$ cycles (compared to the reference solution of 384 cycles) For $h = 0.1$, only 76 cycles have been calculated giving a total fatigue life of $N_R = 392$ cycles.

* CJTV2: For $\eta = 0\ 01$, only 131 cycles have been calculated giving a total fatigue life of $N_R = 387$ cycles. For $h = 0.1$, only 75 cycles have been calculated giving a total fatigue life of $N_R = 391$ cycles It is worth noting that for $h = 0.1$ both computation using CJTV1 and CJTV2 schemes save about 80% of effectively calculated cycles compared to the reference solution, with a very small errors for the total fatigue life (2% for CJTV1 and 1.8% for CJTV2). Moreover, one may see in the figures the effectiveness of the adaptive jump size control in choosing the appropriate size of jump. Large jumps can be seen in regions of low curvature, and progressively, when the curvature of the peak stress curve increases as the material element is close to failure, smaller jumps appear to maintain the accuracy of the prediction.

The accuracy of the simulation with the cycle jump techniques depends obviously on the order of the Taylor development retained to extrapolate the damage variables after the jump. In fact, curves in figure 6 show the response of the same previous simulation with CJTV1 ($\eta = 0.01$) where the damage variable is extrapolated by a first order Taylor expansion The lifetime is then overpredicted with an error of 5.7% which suggests that a higher order extrapolation is suitable to represent the non-linear behavior of the damage variable at the last stage of the lifetime of the material element.

On the other hand, the small time integration scheme has an effect on the cycle jump simulation. This is illustrated by using the classical cycle jump scheme with two different small time integration schemes: asymptotic algorithm (CJTAS) and Runge-Kutta algorithm (CJTRK). All the state variables are involved in the evaluation of the cycle jump step. The cycle jump step associated to a tensorial variable is calculated by using its second invariant. The simulation is then conducted with the same previous loading and parameters, but with a slight change in the material parameters a=5 and b=3 to have a longer non-linear hardening stage and without coupling the damage The results show that the calculations are performed respectively for 141 and 165 cycles with CJTAS and CJTRK, instead of 500 cycles for the full calculation (Figure 7). One may note that the asymptotic

algorithm seems to give a better self-stability to the cycle jump scheme. As a matter of fact, when the prediction deviates after the jump from the reference solution obtained by the full calculation, the redistribution of the state variables occurs more rapidly for the asymptotic algorithm leading to more accurate estimation of the cycle jump step.

Now the case of the non-proportional loading path given in Figure 3b is examined using the same $\eta = 0.1$, which is shown to be enough to estimate the cycle jump increment ΔN. The numerical severity of this type of loading path comes from the fact that the normal to the yield surface changes during the cycle. Three different calculation have been performed with the same loading path using three different cycle jumping schemes. The obtained results are summarized in Table 2 and shown in Figures 8, 9, 10 and 11.

	Predicted lifetime N_R		Number of calculated cycles		Error (%)	
JUMP-MIN	5 cycles	7 cycles	5 cycles	7 cycles	5 cycles	7 cycles
CJTV1	1008	1006	163	168	1 1	0 9
CJTV2	1026	1024	127	169	2 9	2 7
CJTAS	1001	1004	185	180	0 4	0 7

Table 2. *Predicted lifetimes with different schemes*

Figure 8 shows the simulation with the first test performed with CJTV1 and $\eta = 0\ 1$. Good agreement with full calculation is established. The lifetimes predicted with two different values of JUMPMIN 5 and 7 cycles are respectively 1008 and 1006 cycles. These results correspond respectively to 163 and 168 cycles calculations and give errors of 1.1 and 0.9% for N_R in comparison with the reference lifetime value 997 cycles obtained with full calculation. The effect of JUMPMIN may then be important enough to enable the state variables redistribution to take place, and to permit the correct evaluation of the cycle jump step. In the same manner, the second test performed with CJTV2 and $\eta = 0.1$ gives also an acceptable simulation (Figure 9) with maximum error of 2.9 % for N_R. This latter test shows a light difference with the full calculation at the first stage of the lifetime, which reveals the inaccuracy of this kind of extrapolation when the non-linearity of the hardening stage is high. However, the cycle jump scheme is developed specially to simulate a stabilized stage which is the highly consuming CPU time stage and the accuracy can be improved in this region of high curvature using a lower value of the accuracy parameter. On the other hand, one may underline for CJTV1 and CJTV2

the adaptability of the parameters ΔL and D to take into account the multiaxiality of the loading and to estimate the suitable cycle jump step. Finally, the last tests are performed with CJTAS (Figure 10). The simulation is not less accurate, the lifetime is predicted with maximum error of 0.7% corresponding to a calculation of 180 cycles. The lower percentage of the cycle jump and the irregularity of the cycle jump steps for this case highlights the strong difficulty of estimating the cycle jump when several variables are taken into account.

Moreover, with the same loading history, the cycle jump technique CTJV2 is tested with the following damage law parameters: $\gamma = 0.1$, $\Gamma = 20$ and $\eta = 15$, which lead to an important fatigue lifetime of $N_R = 57128$ cycles given by the full calculation. Good agreement between the CJTV2 prediction and the full calculation is obtained The predicted lifetime obtained is $N_R = 57938$ cycles (an error of 1 4%), this result has been carried out by computing only 4752 cycles, with a reduction in computer processing time of approximately 91.7%. This test highlights how much the computational effort required for the cycle jump technique is less than 8.3% of that for the full calculation.

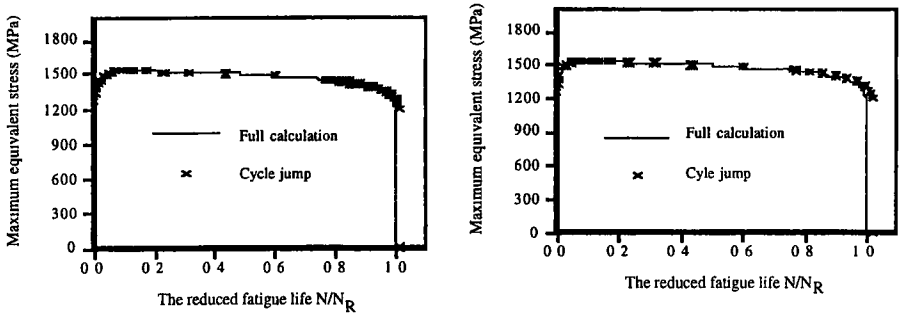

Figure 4. *Simulation for a material element subjected to proportional biaxial loading with CJTV1 and (a) $\eta = 0\ 01$ and (b) $\eta = 0\ 1$*

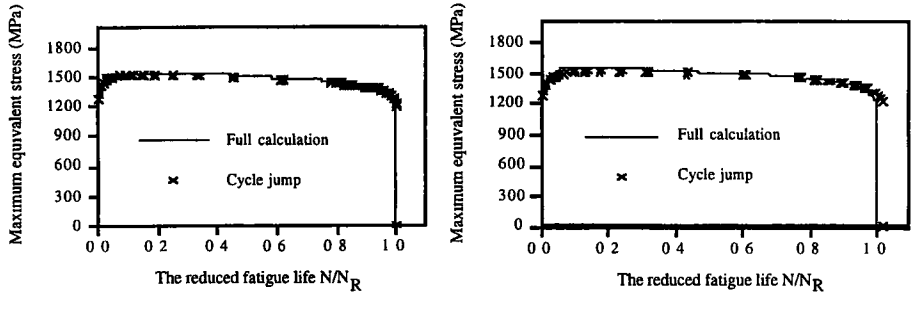

Figure 5. *Simulation for a material element subjected to proportional biaxial loading with CJTV2 and (a) $\eta = 0\ 01$ and (b) $\eta = 0\ 1$*

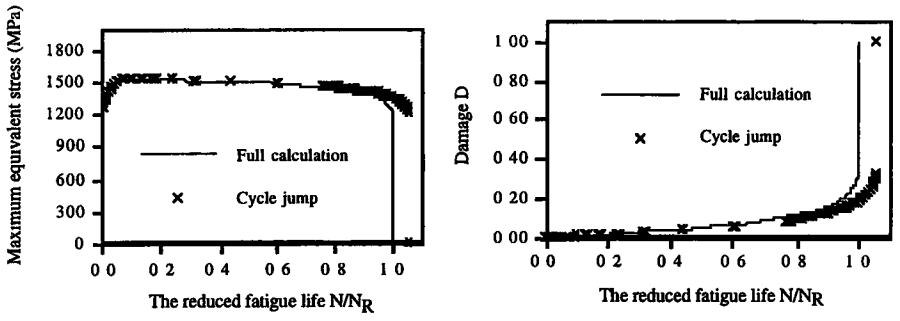

(a) (b)

Figure 6. *Simulation for a material element subjected to proportional biaxial loading with CJTV1 with a first order extrapolation of the damage*

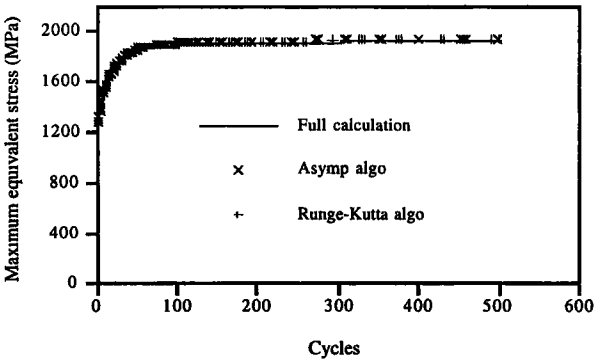

Figure 7. *Effect of the small time integration scheme*

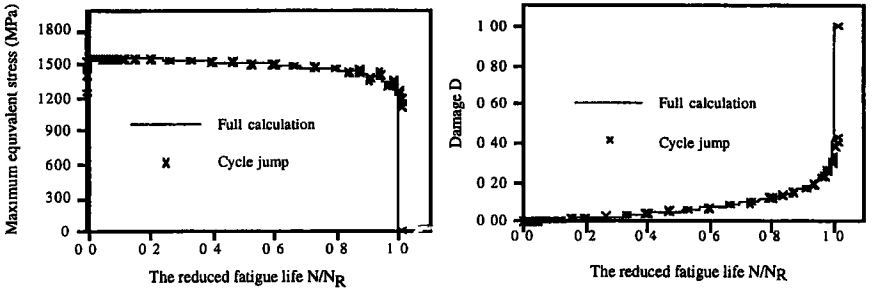

(a) (b)

Figure 8. *Simulation for a material element subjected to non-proportional loading with CJTV1, $\eta = 0\ 1$ and JUMPMIN = 7 cycles*

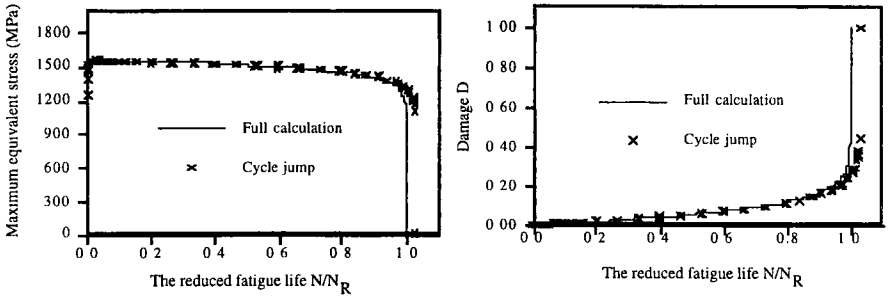

Figure 9. *Simulation for a material element subjected to non-proportional loading with CJTV2, $\eta = 0\ 1$ and JUMPMIN = 7 cycles*

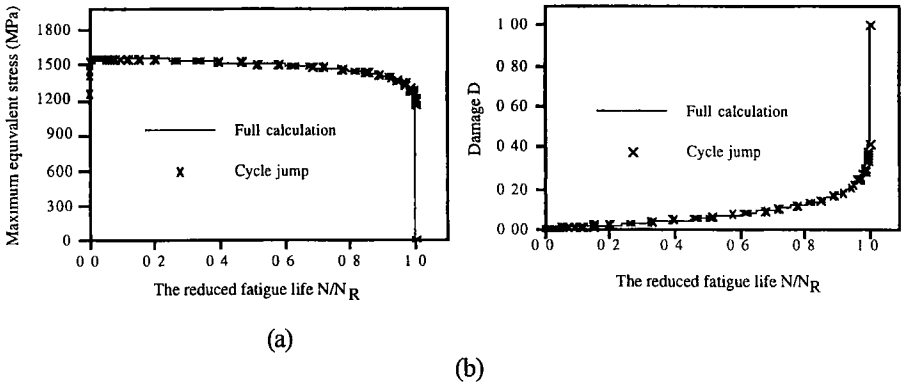

Figure 10. *Simulation for a material element subjected to non-proportional loading with CJTAS associated to the asymptotic algorithm, $\eta = 0\ 1$ and JUMPMIN = 7 cycles*

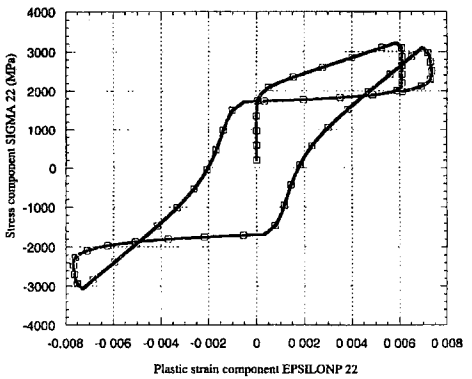

Figure 11. *Hysterersis loop for the studied non-proportional loading path*

Finally, Figure 11 shows the predicted hysteris loop in the space stress-plastic strain for the studied non-proportional path. It is clear that plastic strain amplitude is not so negligeable in this loading path (about 0.8%).

4.2. *At structural level*

The proposed numerical schemes are now discussed in the context of finite element simulation. Both the constitutive equations and numerical schemes are implemented in finite element code SIC (available at the University of Technology of Compiègne). The cycle jump step ΔN is calculated at each Gauss integration point and the retained value is the minimum one among all ΔN over all Gauss points. Two sample problems are included to demonstrate the utility of the numerical schemes: three bars structure and a plate with a circular hole.

4.2.1. *Simplified three bars structure*

The example is composed of three bars with different lengths to reproduce stress concentration (Figure 12). The material coefficients are shown in Table 1, except for the damage law where the coefficients γ and Γ are taken as 0.3 and 10 respectively to have a predicted fatigue life less than 10^3 cycles. Each bar is modeled with an eight node quadrilateral plane strain finite element. A tensile loading performed simultaneously on the three bars induces different fields redistribution in each bar Indeed, in the case of cyclic loading (cycled between ± 0 016 total strain within a period of 64 s), the failure occurs successively in the bars where the stress is more important as shown in Figure 12 The calculation with CJTV2 (η=0 1) is performed for 110 cycles instead of 699 cycles. The number of cycles corresponding to the failure of the three bars is predicted with an error of 1.2%. Moreover, one may see the effectiveness of the adaptive jump size control in choosing the appropriate size of ΔN. As the first bar is close to failure, smaller jumps appear, and as soon as the failure occurs, large jumps can be seen for the simulation of the second bar which is still in its stabilized stage. The same behavior is observed at the failure of the second bar.

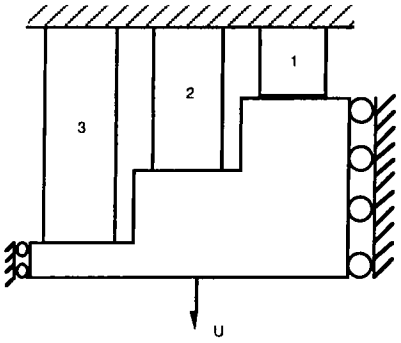

Figure 12. *Simplified three bars structure*

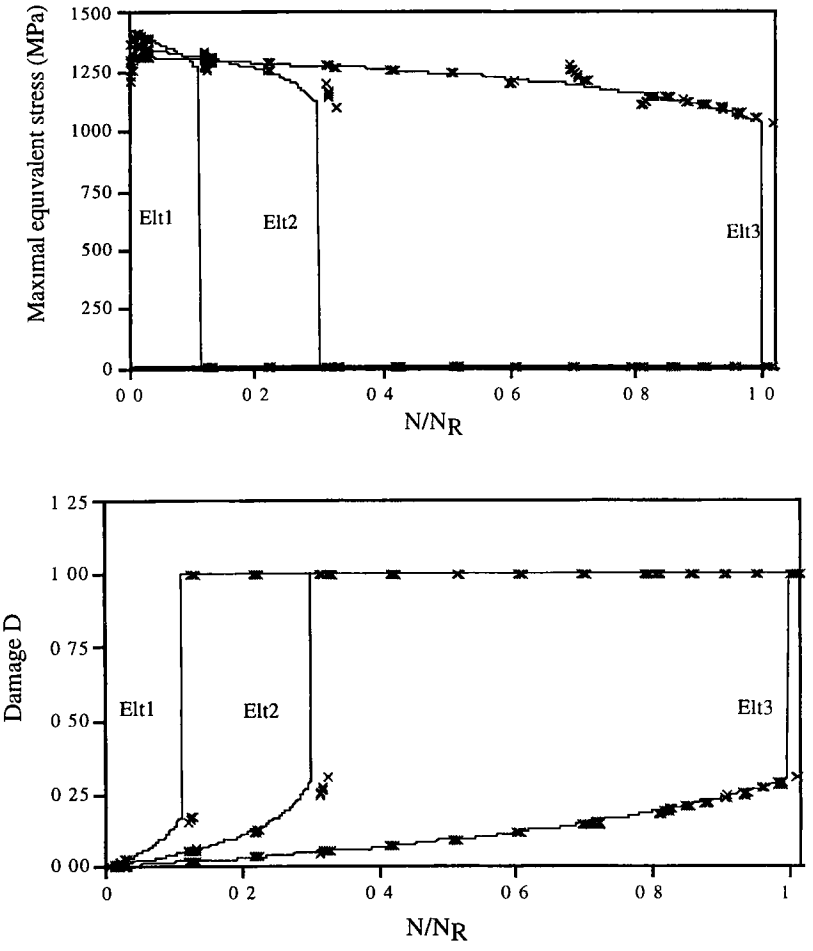

Figure 13. *Behavior of three bars structure subjected to cyclic loading with CJTV2* $\eta = 0\ 1$ *and JUMPMIN = 5 cycles*

4 2.2. *A plate with a central circular hole*

This example concerns a rectangular plate with a circular hole at its center as given in Figure 14. The material coefficients are shown in Table 1, except for the damage law where the coefficients γ and Γ are taken respectively 0.35 and 10. The two opposite ends of the plate are subjected to uniform displacements with no lateral constraints. A complete loading-unloading cycle at a constant strain rate of 0 001/s is applied to the plate within a time period of 28 s. By taking advantage of symmetry, only a quarter of the plate was modeled by 288 a eight-noded plane

strain element Local responses are represented in Figure 15 at the Gauss points A, B and C belonging respectively to elements 277, 217 and 145 The first broken Gauss point belongs to element 277 (Gauss point A). The simulation with CJTV2 reproduces quite accurately the local responses obtained by the full calculation (Error of 2.6% with η=0.1 and only 169 cycles are calculated instead of 615 cycles for the first broken Gauss point). One may note that the variables ΔL and D represent adequately the evolution of the state variables for evaluating the cycle jump step.

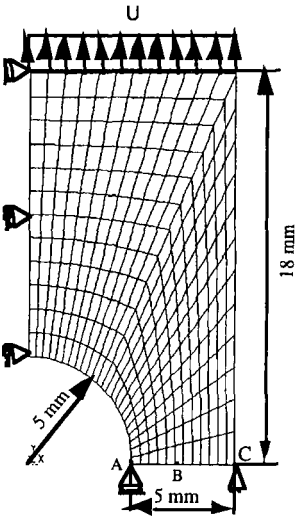

Figure 14. *A plate with a central circular hole*

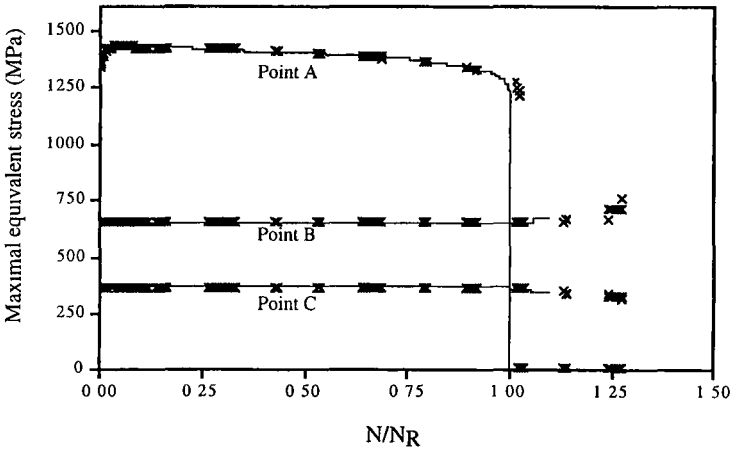

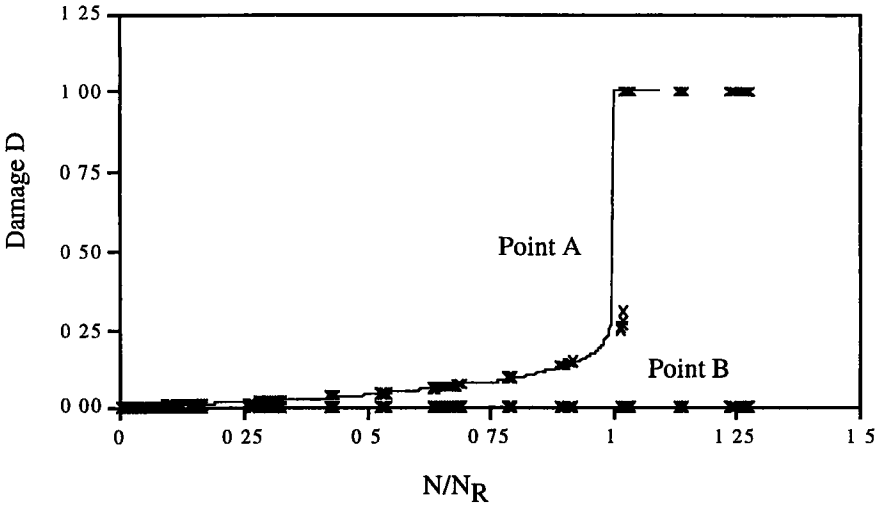

Figure 15. *Simulation of a plate with a circular hole subjected to cyclic loading with CJTV2, $\eta = 0\ 1$ and JUMPMIN = 5 cycles*

5. Conclusion

A two time scale scheme for integrating the coupled damage viscoplastic constitutive rate equations under cyclic loading paths involved in finite element analysis is presented. This resolution strategy uses both implicit and explicit schemes simultaneously in two different time scales. The small time integration scheme is performed with an asymptotic algorithm based on the integral formulation of the constitutive equations and leads to an iterative implicit strategy. The large time integration scheme is explicit and based on the Euler expansion with an adaptive cycle step ΔN calculation. It is found that the combination of the two time scale schemes allows to predict the complete state variables and the correct lifetime with a significant reduction in computer processing time of more then 90%. The selected parameters ΔL and D give an adequate measure of the way in which the state variables redistribution is taking place over the cycles and in addition reduces the number of the stored variables The calculation of the cycle jump step ΔN then becomes more efficient. This two time scale scheme constitutes a helpful engineering tool for the fatigue life prediction using a fully coupled constitutive equation. However, the present damaged viscoplastic model should be improved to take into account the unilateral nature of damage, which is associated with the possibility for the existing microcracks to be open (active damage) or closed (passive damage) by the external applied load.

Acknowledgment

This work was carried out when the authors were in the LG2mS Laboratory at the University of Technology of Compiègne.

6. References

[AKR 97] AKRACHE, R., Lu,J. "Fatigue life prediction for 3D structures", *Computational plasticity, 5th Int. Conf.,* Edit. By DRJ. Owen and al, Barcelona, March 1997.

[AUR 94] AURRICCHIO, F., TAYLOR, R.L , "A generalized elastoplastic plate theory and its algorithmic implementation", *Int. J Numer Methods Engrg.* 37, 2583-2608, 1994

[BEN 81] BENALLAL, A, « Prévision de l'amorçage en fatigue à chaud », Thèse Docteur Ingénieur, Université Paris 6, 1981.

[CHA 77] CHABOCHE, J.L « Sur l'utilisation des variables d'état interne pour la description de la viscoplasticité cyclique avec endommagement », Problèmes non linéaires de mécanique, Cracovie. pages 137-159, 1977, *Symp Franco-Polonais de Rhéologie et Mécanique,* 1977

[CHA 78] CHABOCHE, J L , « Description thermodynamique et phénomonologique de la viscoplasticité cyclique avec endommagement », Thèse de Doctorat Es-Science, Paris VI, 1978

[CHA 86] CHABOCHE, J L , CAILLETAUD, G , « On the calculation of structures in cyclic plasticity or viscoplasticity », *Comp. Struct.* 23, (1986), 23-31.

[CHA 96] CHABOCHE, J.L., CAILLETAUD, G., "Integration methods for complex plastic constitutive equations", *Comput. Methods Appl Mech. Engrg* 133 (1996) 125-155, 1996.

[CHU 91] CHULYA, A , WALKER, K.P. "A new uniformly Valid Asymptotic Integration Algorithm for Elasto-plastic creep and Unified Viscoplastic Theories including continuum damage", *Int Journal for Num. Meth in Eng ,* Vol.32, pp 385-418 1991

[DUN 94] DUNNE F.P E., and HAYHURST D.R., "Efficient cycle jumping techniques for the modelling of materials and structures under cyclic mechanical and thermal loading", *Eur J. Mech. A/Solids* 13, n°5, 639-660, 1994.

[FRED 92] FREED A D , WALKER K.P, "*Exponential Integration algorithms applied to viscoplastitcity*", NASA TM 104461, 3rd Int Conf. on Computational Plasticity, Barcelona, 1992

[GEA 81] GEAR G W , *Numerical initial value problems in ordinary differential equations,* Prentice-Hall, Englewood Cliffs NJ, 1981

[GOL 89] GOLINVAL J C, Calcul par éléments finis des structures élasto-viscoplastiques soumises à des chargements cycliques à haute température, Thèse de Doctorat, Université de Liège, Belgique, 1989

[GUE 86] GUENNOUNI T., AUBRY D , *Réponse homogénéisé en temps de structures sous chargements cycliques*, CRAS, tome 303, série II, pp 1765-1768, 1986

[HAM 00] HAMMI Y , Simulation numérique de l'endommagement dans les procédés de mise en forme, Thèse de Doctorat de l'Université de Technologie de Compiègne, 2000

[LAD 85] LADEVÈZE P , *Sur une famille d'algorithmes en mécanique des structures*, CRAS, 300, série II, n°2, pp.41-44, 1985.

[LEM 86] LEMAITRE J , "*Local approach of fracture*", *Eng Fract. Mech.*, Vol 25, n° 5/6, p 523, 1986.

[LEN 89] LESNE, P.M., SAVALLE S., "*An efficient cycles jump technique for viscoplastic structure calculations involving large number of cycles*", *Second Inter Conference on Computational Plasticity*, pp. 591-602, Barcelona., 1989.

[NES 96] NESNAS K., BEN HATIRA F., BEZZINA S., SAANOUNI K., "*On some integration schemes for rate equations of damaged elastoplastic model*", *Revue Européenne des éléments finis*, Vol 5, n°4/1996.

[NES 98] NESNAS K., Sur des méthodes numériques de calcul des structures sous chargement cycliques, Thèse de Doctorat de l'Université de Technologie de Compiègne, 1998

[NES 00] NESNAS K , SAANOUNI K., « An integral formulation of coupled damage and viscoplastic constitutive equations: Formulation and Computational issues », submitted to *Int J of Damage Mechanics*

[SAA 94] SAANOUNI K., Ben HATIRA F., FORSTER CH , "On the Anelastic flow with damage", *Inter. J. Damage. Mech*, vol. 3, 140-169 1994.

[SIM 86] SIMO J.C., and TAYLOR R.L., "A return Mapping Algorithm for plane stress Elastoplasticity", *Inter. J. Num. Methods. Eng.*, 22, 649-670. 1986

[TOU 93] TOUZOT G , DABOUNOU J., « Intégration numérique de lois de comportement élastoplastique », *Revue Européenne des éléments finis*, vol. 2, p. 465-492. 1993

[WAL 87] WALKER K P, "A uniformly valid asymptotic integration algorithm for unified viscoplastic constitutive models", in: S. Nakazawa et a , eds., *Advances in Inelastic Analysis*, AMD. Vol. 88 1 PED. Vol. 28 (ASME, 1987) 13-27, 1987